ISSN: 2710-0588

Research on Seismic Performance of The Pre-stressed Rocking Bridge Pier with Variable Friction Self-centering Damper System

Pengfei Zhao

College of Civil Engineering, Henan Polytechnic University, Jiaozuo 454000, Henan, China

Abstract

Objectives: In order to enhance the hysteretic energy dissipation capacity of the unbonded prestressed concrete swing abutment bridge under seismic action, a study on the reliability of a variable friction self-resetting damper to improve the energy dissipation capacity of the unbonded prestressed concrete swing abutment bridge is proposed. Methods: The force-displacement relationship of the enhanced rocking bridge pier with variable friction self-resetting dampers was calculated by using theory and finite element method. The consistency of the results obtained by the two methods was evaluated. Three parameters, namely the initial tension stress of the prestressed tendons, the stiffness of the lateral compression spring of the dampers, and the friction coefficient of the dampers, were analyzed. The influence of these parameters on the seismic performance of the enhanced rocking bridge pier system with variable friction self-resetting dampers was studied. Results: When only the initial tensioning stress of the prestressed steel strands is changed to increase it from 800 MPa to 900 MPa, the maximum restoring force increases by 3.5%, the equivalent damping ratio at the maximum displacement of the structure decreases by 5.4%, and the energy consumption increases by 4.3%. When the initial tensioning stress is changed from 900 MPa to 1000 MPa, the maximum restoring force increases by 5.4%, the equivalent damping ratio at the maximum displacement of the structure decreases by 79%, and the energy consumption decreases by 70%. When only the lateral compression spring stiffness of the damper is changed to increase it from 80 kN/mm to 100 kN/mm, the maximum restoring force increases by 3.2%, the equivalent damping ratio at the maximum displacement of the structure increases by 2.7%, the stiffness after yielding increases by 1.7%, and the energy consumption increases by 0.51%. When the spring stiffness of the damper is changed from 100 kN/mm to 120 kN/mm, the maximum restoring force increases by 2.2%, the equivalent damping ratio at the maximum displacement of the structure increases by 0.27%, the stiffness after yielding increases by 1.8%, and the energy consumption increases by 2.5%. When only the friction coefficient of the damper is changed to increase it from 0.2 to 0.23, the maximum restoring force increases by 0.23%, the equivalent damping ratio at the maximum displacement of the structure decreases by 0.6%, the energy consumption value increases by 3.6%, and the residual displacement increases by 9.9%. When the friction coefficient of the damper is changed from 0.23 to 0.25, the maximum restoring force increases by 0.87%, the equivalent damping ratio at the maximum displacement of the structure decreases by 0.2%, the energy consumption value increases by 0.67%, and the residual displacement increases by 5.5%. Conclusions: When the initial tension stress applied to the prestressed tendons is 0.45 times their own yield strength, the spring stiffness of the damper is 120 kN/mm, and the friction coefficient is 0.25, the system has good energy dissipation and self-centering performance. The research results are relatively reliable.

ISSN: 2710-0588

Keywords

Ampers; finite element analysis; initial tensioning stress; spring stiffness; friction coefficient.

1. Introduction

Bridge piers are important load-bearing components of bridges, and their mechanical properties have a significant impact on the safe operation of bridges. Multi-column frame piers are the most commonly used pier form in bridges at present. Frame piers designed based on ductility can meet the seismic defense requirements of "no damage in minor earthquakes, repairable in moderate earthquakes, and no collapse in major earthquakes", but they will experience significant residual deformation under strong earthquakes[1], becoming standing ruins. For example, in the 1995 Kobe earthquake[2], more than 100 piers were demolished due to residual deformation exceeding 1.0%. Therefore, reducing post-earthquake residual deformation has become an important way to improve the seismic resilience of bridges.

In 1974, Beck [3] first conducted research on the combined application of the rocking concept and bridge seismic design, and the research results were reflected in the design of the South Rangitikei Railway Bridge in New Zealand[4]. Subsequently, Astanen-Asl [5] carried out the seismic retrofit design of the San Francisco-Oakland Bay Bridge in the United States and proposed the implementation of semi-rigid connections between the piers and the foundation, which could allow limited rocking under seismic action. This connection mechanism limits the seismic force transmitted to the superstructure and reduces the damage of the structure under seismic action.

Although unbonded prestressed rocking piers will experience a certain degree of rocking under seismic loads, the tensile deformation of the prestressed tendons will restore the components to their original position, thereby ensuring that the pier columns are not damaged under seismic action. However, unbonded prestressed rocking piers have almost no energy dissipation capacity. By adding energy dissipation devices to the rocking piers, not only can seismic energy be dissipated, but the self-recovery capacity of the rocking piers can also be further enhanced, thereby reducing residual displacement. Jin Shuangshuang [6]proposed an external replaceable energy dissipation steel plate to enhance the energy dissipation capacity of the piers. Gu Shuo [7] used a viscoelastic damper externally attached to the prestressed tendon assembled pier to improve the energy dissipation capacity of the self-recovering pier. The above research results show that the flag-shaped hysteretic relationship of the piers becomes more full after adding energy dissipation devices, and the hysteretic energy dissipation capacity is significantly enhanced[8]. The use of friction dampers or BRBs and other metallic energy dissipation dampers can also significantly enhance the energy dissipation capacity of rocking piers. Liu Xirui[9] proposed a seismic isolation device with a durable damper and a buckling-restrained brace (BRB) in parallel for continuous arch bridges and further verified the feasibility of the seismic mitigation measures. Liu Yanfang[10] proposed a seismic mitigation device composed of a self-recovering spring, a friction rope, and a friction shaft to be added to continuous bridges to improve seismic resistance, effectively enhancing the seismic mitigation performance of continuous bridges.

In recent years, different types of friction self-recovering devices have been proposed. The damper composed of disc springs and friction energy dissipation devices can achieve strong seismic mitigation effects in a small space. Xue[11] et al. and Hashemi[12] et al. proposed a new recoverable sliding friction (RSF) damper composed of a wave-shaped outer plate, a slotted inner plate, high-strength bolts, and disc springs. Xu Longhe[13] et al.used pre-compressed disc springs and friction elements to form a disc spring-based self-recovering damper. Yu Tianhao[14]et al. proposed a seismic mitigation device combining a disc spring and a U-shaped

ISSN: 2710-0588

damper to solve problems such as low energy dissipation under low pre-compression displacement.

Among the above dampers, the disc springs, springs, and other recovery elements have the dual functions of providing surface normal pressure and recovery force to the friction elements. This combination makes these self-recovering friction dampers more compact in structure. In addition, the friction force of these dampers increases with the increase in deformation, which is called a variable friction self-recovering damper. This feature enables their energy dissipation capacity to increase with the increase in seismic intensity.

In this paper, a variable friction self-recovering damper is added to the unbonded prestressed rocking pier to improve the energy dissipation capacity and self-recovery performance of this type of pier. Theoretical derivation was conducted to obtain the force-displacement relationship skeleton curve of the rocking double-column pier enhanced by the variable friction self-centering damper. Meanwhile, the force-displacement hysteretic curves of the pier under cyclic loading were calculated by finite element method, and the calculation results obtained by the two methods were compared. Subsequently, parametric analysis was carried out to obtain the influence laws of key parameters on the hysteretic energy dissipation and self-centering performance of the pier. The obtained results provide a reference for the design of the rocking pier enhanced by the variable friction self-centering damper.

2. Enhancing the Swing Bridge Pier Structure with Friction Self-resetting Dampers

In this study, a new type of variable-friction self-resetting energy dissipation dampers were adopted in combination with prestressed oscillating pier to form an enhanced oscillating pier bridge with friction self-resetting dampers.

The structure of the adopted variable friction self-resetting damper is shown in Figure 1(a). It mainly consists of symmetrically arranged V-shaped friction plates, wedge-shaped sliders, transverse compression springs, transverse guide tubes, left/right side frames, and actuating rods. The upper/lower V-shaped friction plates and left/right side frames in the variable friction self-resetting mechanism are connected by high-strength screws. Initially, the wedge-shaped surface of the wedge-shaped slider matches the vertex of the V-shaped sliding groove of the friction plate. A transverse compression spring is set between the two sliding blocks, and the two sliding blocks and the compression spring are externally equipped with guiding cylindrical tubes. The two sliding blocks can freely slide along the axial direction within the guiding cylindrical tubes. When the actuating rod is pulled, the sliding blocks at both ends of the sleeve gradually shorten under the inclined surface guidance, and the spring in the transverse guide tube is compressed. The positive pressure and friction force generated by the compression spring in the direction of the actuating rod movement are the damping force provided by this damper; when the external force is removed, under the squeezing effect of the inclined surface, the wedge-shaped slider, guide tube and actuating rod move in the opposite direction, and at the same time, a restoring force is generated. The magnitude of the restoring force is equal to the algebraic sum of the positive pressure and the friction force on the inclined surface in the direction of motion.

The pre-stressed tendons swaying bridge piers are shown in Figure 1(b). The main components include the main girder, pier column, unbonded prestressed tendons, etc. Compared with traditional cast-in-place bridges, the swaying bridge piers are equipped with dry joints between the upper structure and the abutment, and the unbonded prestressed tendons running through them connect them into a whole. The contact surfaces' opening and closing are utilized to meet the structural displacement requirements. Under the action of earthquakes, a swaying interface is formed at the joint between the pier top and bottom[15]. Through the continuous "opening"

ISSN: 2710-0588

and "closing" of the connection part, energy is dissipated, and the structural damage is controlled at the swaying interface.

In the self-resetting damping device enhanced sway bridge piers, the two ends of the damping device are respectively connected to the bottom of the pier column and the foundation through pins, as shown in Figure 2(c). Under the action of earthquakes, the variable friction self-resetting damping device deforms along with the lateral sway of the pier column. At this time, both the variable friction self-resetting damping device and the prestressed steel bars in the pier column provide restoring forces for the pier column. The force-displacement relationship diagram of the sway pier, the variable friction self-resetting damping device and the self-resetting damping device enhancing the sway pier is shown in Figure 2. The variable friction self-resetting damping device itself has strong energy dissipation capacity and certain self-resetting ability. When it is combined with the sway pier, it can enhance the energy dissipation capacity of the pier column while not affecting or even enhancing the self-resetting ability of the pier column.

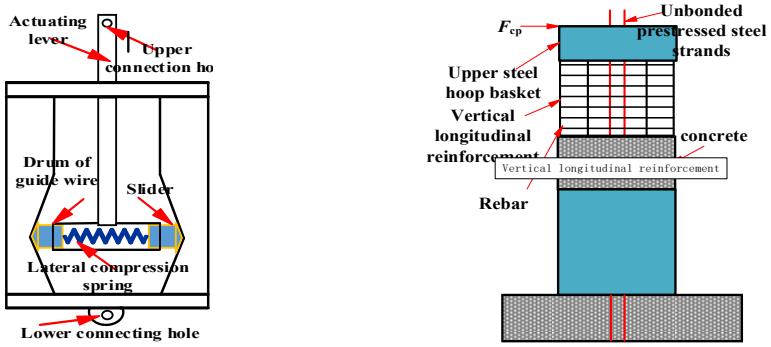

(a) Variable friction self-resetting damper (b) Prestressed reinforcement swing pier

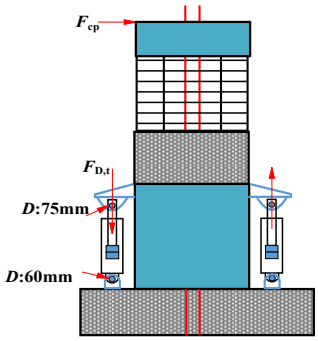

(c) Self-resetting damping-enhanced oscillation pier

Figure 1. Pre-stressed rocking pier enhanced with variable friction self-centering dampers

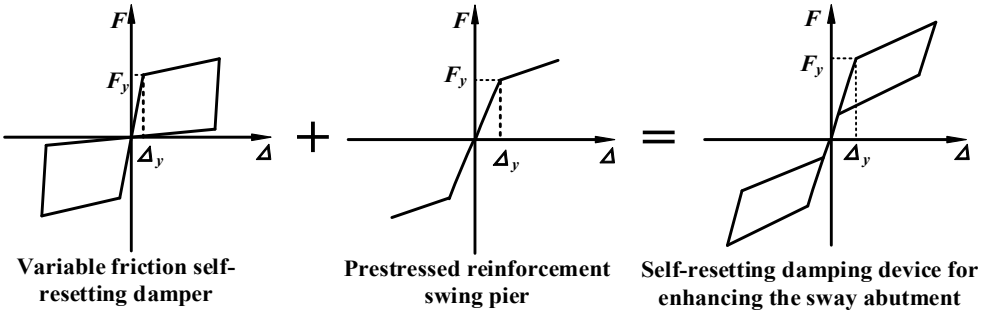

Figure 2. Force-displacement relationship of rocking pier with variable friction self-centering dampers

ISSN: 2710-0588

3. Derivation of Force-Displacement Relationship

The restoring force of the oscillating pier enhanced by the self-resetting dampers is jointly provided by the prestressed tendons and the dampers. To facilitate the derivation of the force-displacement relationship of the oscillating pier enhanced by the self-resetting dampers, the following assumptions are made:

(1) The outer frame of the friction self-resetting damper is a rigid body.

(2) When the piers do not sway, under the action of their own weight and the upper loads, the bottom surfaces of the pier columns are completely in contact with the ground.

(3) During the swaying process, the deformation of the piers always remains within the linear elastic range. As shown in Figure 3, when the lateral force is sufficiently large, the pier column will rotate around the bottom "O" point. The rotation angle "θ" increases as the lateral displacement of the pier column increases. At this time, the angle between the bottom surface of the pier column and the ground is also "θ". When the magnitude and direction of the lateral force change with time, the pier column will sway. During the swaying process, the pier column will cause the prestressed steel bars and dampers to deform, and the pier column will simultaneously receive the restoring forces provided by both.

When the moment generated by the lateral force acting on the pier exceeds the moment that can be overcome by the initial stress of the prestressed steel strands, the pier column will open at the swaying interface and will drive the prestressed steel strands within it to deform. The prestressed steel strands will generate an anti-overturning moment, which increases accordingly. After the external force is removed, the pier column will recover to its initial state under the action of the prestressed steel strands and achieve self-resetting.

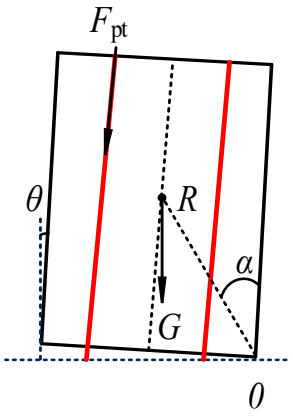

(a) Diagram showing the rotation of prestressed steel strands

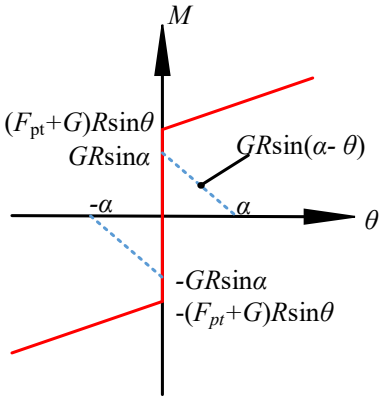

(b) Bending moment-rotation angle skeleton curve

Figure 3. Aslam model[16]

ISSN: 2710-0588

When the bridge piers are subjected to lateral forces but do not sway, the lateral loads are borne by the pier columns, and the bending stiffness of the columns is expressed as:

$$K_c=n_c\times\frac{12E_cI}{H} \tag{1}$$

In the formula: n_c represents the number of bridge piers, H is the net height of the bridge piers, E_c is the elastic modulus of the bridge piers, I is the moment of inertia of the interface of the bridge piers. is the moment of inertia of the interface of the bridge piers.

$$\Delta=\Delta_\theta+\Delta_f \tag{2}$$

In the formula: Δ For the total lateral displacement of the bridge piers， Δ_f For the displacement caused by the deformation of the bridge piers, Δ_θ the displacement caused by the oscillation and rotation angle of the bridge piers. During the swaying process of the piers, the height of the compression zone is not taken into account. The bottom of the pier body opens and closes relative to the cap, and the resulting angle is:

$$\theta=\frac{\Delta_\theta}{H} \tag{3}$$

In the formula: H It is the net height of the pier column. In theoretical calculations, the internal forces generated by each prestressed steel strand are as follows:

$$\mathrm{Fpt=EsAs[}\frac{\mathrm{(bb+bt)\times\theta}}{\mathrm{Lp}}\mathrm{+\varepsilon 0]} \tag{4}$$

In the formula: F_{pt} it is the net height of the pier column. In theoretical calculations, the internal forces generated by each prestressed steel strand are as follows: E_s the elastic modulus of prestressed steel strands; A_s For the cross−sectional area of prestressed steel bars; L_p The length of the non-adhesive section of prestressed steel strands; b for the width of the bridge piers; b_t half of the upper width of the bridge piers、 b_b Half of the width of the lower part of the bridge piers; θ the angle caused by the swaying of the bridge piers; ε_0 For the initial strain of prestressed reinforcement.

Figure 4 shows the mechanical model of the additional system. It is obvious that the dampers located farther away from the rotation center "O" are under tension, while those closer to "O" are under compression. According to the geometric relationship, it can be known that:

$$L_{D,t}=b+d \tag{5}$$

$$L_{D,c}=b \tag{6}$$

In the formula: $L_{D,t}$ the distance from the center of the bottom of the tension-side damper to the rotation center, $L_{D,c}$ the distance from the center of the bottom of the compression damper to the rotation center, d the distance from the center of the upper pin hole of the actuator lever of

ISSN: 2710-0588

the damper to the root of the connecting component. List the bending moment equilibrium equation, and it can be known that the force-displacement formula of the additional system is as follows:

$$(F_{pt}+\frac{W}{2})(b-\Delta-\frac{c_b}{2}-\frac{c_t}{2})+G(\frac{b}{2}-\frac{c_b}{2}-\frac{\Delta}{2})-F_{cp}[H+(b-c_b-c_t)\sin\theta]+F_{D,t}L_{D,t}+F_{D,C}L_{D,c}=0 \quad (7)$$

In the formula:F_{pt} the prestress provided when the prestressed reinforcement elongates;W The self-weight of the upper components of the bridge piers and the bridge deck load;b for the width of the bridge piers; c_t the half-width of the contact surface between the bridge pier and the bottom of the bridge deck when it sways、 c_b the half-width of the contact surface between the bridge piers and the bottom bearing platform when they sway due to the action of wind or other external forces; G For the self-weight of the bridge piers; H Net height of the bridge piers; θ the angle caused by the swaying of the bridge piers; $F_{D,t}$ the damping force generated by the damper on the tensioned side; $F_{D,c}$ the damping force generated by the damping device on the compressed side.

During the swaying process, the relationship between the swaying angle of the bridge piers and the displacement generated by the dampers is as follows:

$$u = \theta \times L_D \quad (8)$$

From Equations (3) and (8), it can be known that the relationship between the displacement generated by the damper and the displacement resulting from the oscillation of the pier is as follows:

$$u = \frac{\Delta_\theta \times L_D}{H} \quad (9)$$

The force-displacement relationship of the damper is as follows:

$$F_D = \frac{2k|u|\tan\beta[\mathrm{sgn}(u)\mu + \tan\beta]}{1 - \mathrm{sgn}(u)\mu\tan\beta} \quad (10)$$

In the formula: k the lateral spring stiffness of the damper; u Indicating the relative displacement at both ends of the damper; sgn( )it is the sign function.,When sgn $(u) = 1$ it indicates the process of damper loading, when sgn $(u) =$ -1 it indicates the process of damper disengagement;β the inclination angle of the damper's inclined plane; μ indicate the coefficient of friction on an inclined plane; L_D the distance between the damper and the rotation center，This includes $L_{D,t}$ and $L_{D,c}$, It is obtained from formulas (5) and (6).

Figure 5 shows the comparison curves of theoretical, experimental and simulation results of the self-resetting variable friction damper. It can be seen that the curve drawn by the formula of the hysteretic curve derived from the theoretical analysis is basically consistent with the hysteretic curve obtained from the experiments and numerical calculations in terms of the trend of variation.

ISSN: 2710-0588

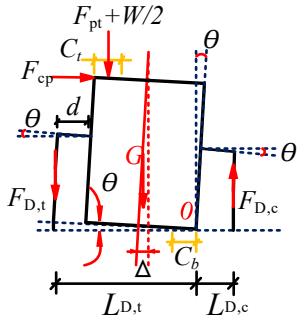

Figure 4. Force analysis of piers reinforced by a single self-resetting friction damper

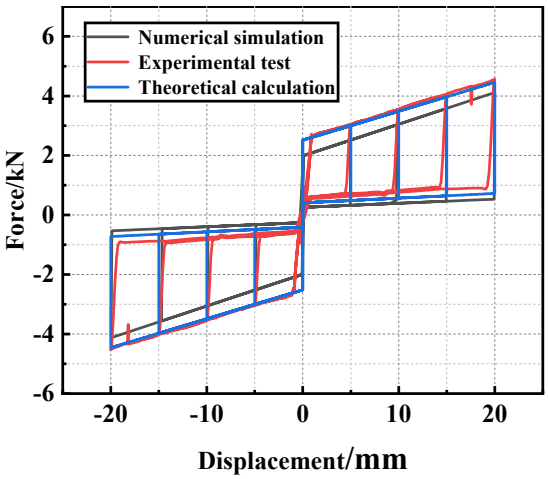

Figure 5. Comparison of hysteresis curves of dampers

4. Finite Element Analysis

This section employs the finite element method to study the mechanical characteristics of the double-column swaying abutment enhanced by the variable friction self-resetting damper. The finite element results are compared with the theoretical analysis results in Section 2. The friction self-resetting damper used to enhance the double-column swaying bridge abutment is shown in Figure 4. The bridge deck width is 10.1m, the abutment height is 5.9m, and the bottom foundation slab size is 11m × 1.5m × 1.5m. The abutment, abutment column, and bottom foundation slab are all cast with C30 concrete, and the stirrups of the abutment columns are composed of grade 8 steel with a diameter of 8mm and are arranged at intervals of 90mm. The vertical longitudinal bars consist of 6 grade 16 steel bars; they are arranged in a circumferential direction from the upper surface of the abutment column to the lower surface, with a protection layer thickness of 50mm. Each abutment column is equipped with 4 prestressed steel strands with a yield strength of 1860 MPa, arranged in a centrosymmetric manner. The prestressed strands pass through the cap beam to the bottom of the foundation slab and are anchored at both ends. To prevent stress concentration, steel hoops are set on the top and bottom surfaces of the abutment columns to improve the compressive strength.The lateral spring stiffness is set at 120 kN/mm.

On the upper part of the actuator lever and the lower part of the external frame, respectively, there are pin holes. The upper part of the damper is connected to the pier body through the pin holes of the actuator lever and the connecting component, and the lower part is connected to the bottom foundation slab through the pin holes of the external frame and the connecting component. The damper is symmetrically arranged on both sides of each pier column.

ISSN: 2710-0588

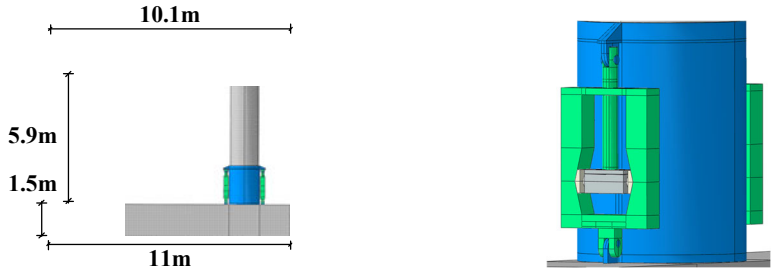

(a) Overall structure diagram (b) Installation of dampers

Figure 6. Structure diagram of double column rocking pier reinforced by friction self-resetting damper

The finite element model of the double-column swing abutment with self-resetting friction damping device is shown in Figure 6. In the simulation, the concrete members, upper steel pad plates, lower steel hoops, damping device connection components, and prestressed steel strands are all established using solid elements, with the element type being eight-node linear hexahedral element (C3D8R). The stirrups and longitudinal bars of the abutment are simulated using two-node linear three-dimensional truss elements (T3D2).

Each component of the damper is established using solid elements, with the element type being the eight-node linear hexahedral element (C3D8R); the material is Q345 steel. The lateral spring simulation is set up using the "axial connection" module in the interaction module, respectively at the center points of the left and right sliders, establishing a straight line in the horizontal direction, connecting the two center points through this line, and assigning this line an elastic stiffness. The slider and V-shaped track, the slider and the cylinder, and the actuating rod and the damper frame all adopt face-face contact. Tangential contact is set as "penalty" friction, and normal contact as "hard" contact. The friction coefficient between the slider and the track is 0.2. The friction coefficient between the slider and the cylinder is 0.01. The friction coefficient between the actuating rod and the frame is 0.2. A control point is set at the top of the actuating rod, and point-face coupling is adopted.

The displacement loading mode is a horizontal reciprocating loading. The amplitude curve input method is adopted. A reference point is set at the center of the bridge deck, and the reference point is coupled with the bridge deck. The displacement is applied to the reference point. The loading levels are ±5mm, ±10mm, ±20mm, ±30mm, ±40mm, ±50mm, ±60mm, and ±70mm. Each level is loaded once in a cycle.

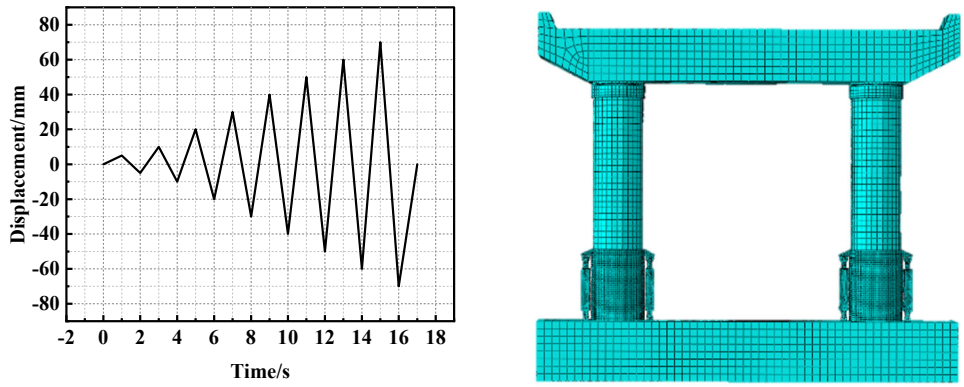

Figure 7. loading path and Finite element model

Based on the force-displacement formula of the additional system derived in Section 2, through theoretical calculation, the skeleton curves of the model under monotonic and reciprocating loading conditions can be obtained. In this case, the parameter values in each formula are the

ISSN: 2710-0588

same as those set in the numerical model. The comparison between the skeleton curves obtained by theory and those calculated numerically is shown in Figure 8.

The results show that the yield force obtained from theoretical calculation differs by 17% from that obtained from numerical calculation, while the maximum recovery force derived from theoretical calculation differs by 18% from that obtained from numerical calculation. The trend of the force-displacement skeleton curve derived from theoretical formula is basically consistent with the numerical simulation results.

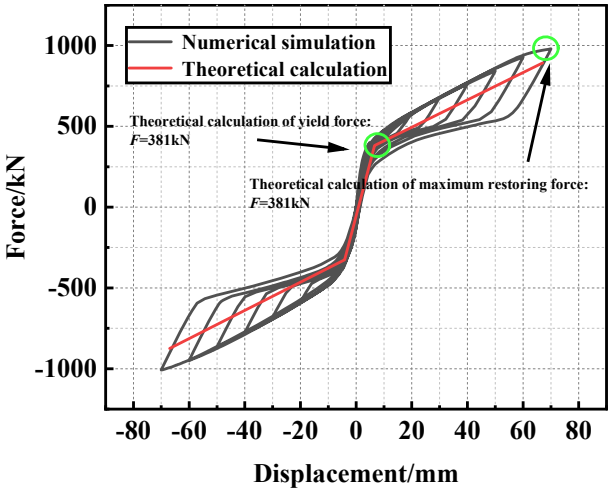

Figure 8. Numerical and theoretical comparison of the addition of dampers and swing piers

The main factor leading to the difference between the two is that there are certain differences between the finite element model calculation model and the theoretical derivation model in terms of the model itself and the actual situation. For example, in the finite element calculation, the mesh division, boundary and contact surface settings, as well as the rigid assumption of the pier column and damper frame in the theoretical calculation, etc.

Figure 9 compares the mechanical properties of prestressed double-column piers and friction self-resetting damper enhanced double-column piers. Figure 9(a) shows that compared with the prestressed double-column piers, the hysteresis curve of the friction self-resetting damper enhanced double-column piers is significantly fuller, which makes the restoring force of the original prestressed steel strand double-column swaying piers larger, and Figure 9(b) shows that under the enhanced effect of the damper, the hysteretic energy dissipation capacity is significantly improved.

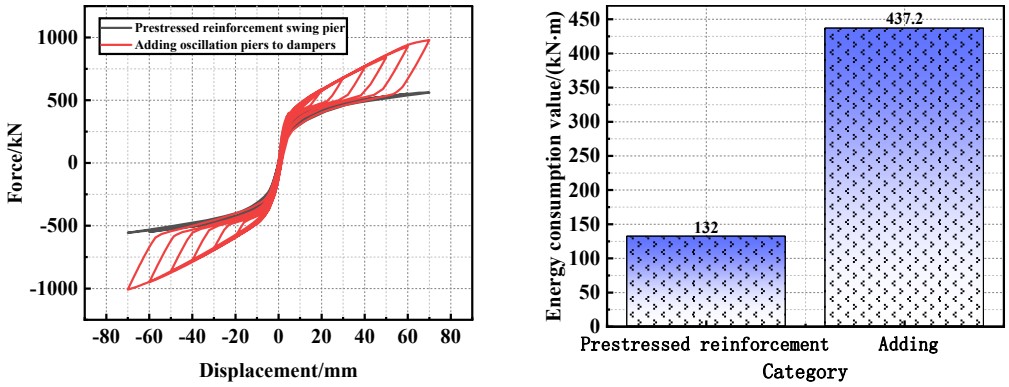

(a) Hysteresis loop comparison (b) Comparison of total energy consumption values

Figure 9. Dampers enhance the contrast of rocking piers

ISSN: 2710-0588

5. Parametric Research

The prestress of the prestressed reinforcement, the lateral spring stiffness and friction coefficient of the self-resetting friction damper are the three key parameters that affect the self-resetting damper in enhancing the mechanical properties of the double-column oscillating pier. This section mainly discusses the influence laws of these three parameters on the mechanical properties of the double-column reinforced by the self-resetting damper.

5.1. The influence of the initial tensioning stress

Figure 10 shows the force-displacement curves, equivalent damping ratios, stress-strain curves of prestressed tendons and the amount of energy dissipated during cyclic lateral loading of the bridge pier under different displacement amplitudes when the lateral spring stiffness of the damper is set at 120 kN/mm and the friction coefficient between the slider and the inclined plane is 0.2. The initial tension stress P of the prestressed tendons is 800 MPa, 900 MPa and 1000 MPa respectively.

When the initial tensile stress increased from 800 MPa to 900 MPa, the maximum restoring force increased by 3.5%, the equivalent damping ratio at the maximum displacement of the structure decreased by 5.4%, and the energy consumption increased by 4.3%. When the initial tensile stress increased from 900 MPa to 1000 MPa, the maximum restoring force increased by 5.4%, the equivalent damping ratio at the maximum displacement of the structure decreased by 79%, and the energy consumption decreased by 70%. Under the three working conditions, the maximum stress of the prestressing steel was all less than the yield strength of 1860 MPa, and the prestressing steel could play a good self-resetting role.

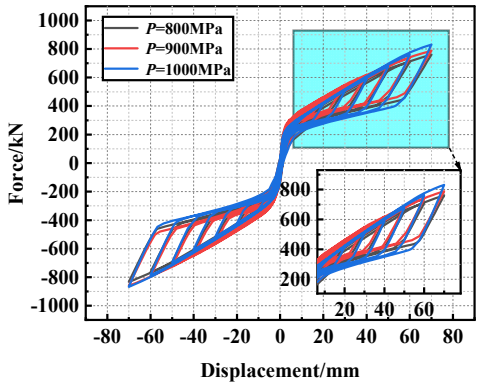

(a) Hysteresis loop

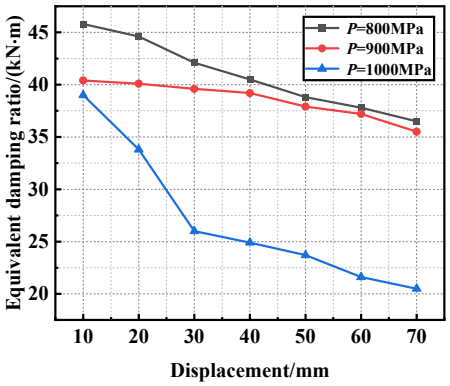

(b) Equivalent damping ratios

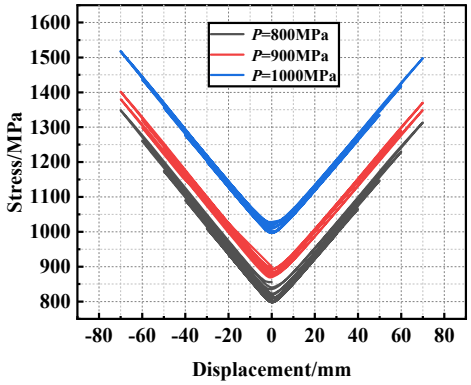

(c) Variation of prestressed steel stress with displacement

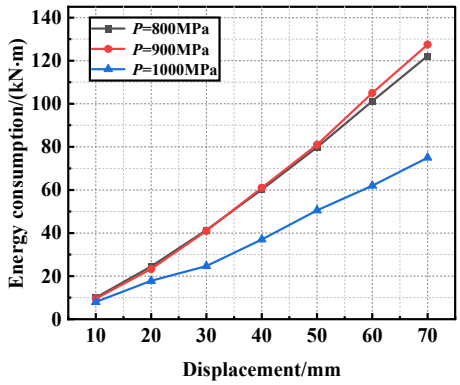

(d) Comparison of energy consumption

Figure 10. Comparison of various parameters under different initial tensile stresses

ISSN: 2710-0588

5.2. The influence of the stiffness of the lateral compression spring

Figure 11 shows the force-displacement curves, equivalent damping ratios, skeleton curves and hysteretic energy dissipation of the bridge piers under lateral cyclic loads at different displacement amplitudes when the initial tension stress of the prestressed tendons is 850 MPa and the friction coefficient of the damper is 0.2. The lateral spring stiffness k of the damper is 80 kN/mm, 100 kN/mm and 120 kN/mm respectively.

When the spring stiffness increases from 80 kN/mm to 100 kN/mm, the maximum restoring force increases by 3.2%, the equivalent damping ratio of the structure increases by 2.7% at the maximum displacement, the yield stiffness increases by 1.7%, and the hysteretic energy dissipation increases by 0.51%. When the spring stiffness of the damper increases from 100 kN/mm to 120 kN/mm, the maximum restoring force increases by 2.2%, the equivalent damping ratio of the structure increases by 0.27% at the maximum displacement, the yield stiffness increases by 1.8%, and the hysteretic energy dissipation increases by 2.5%.

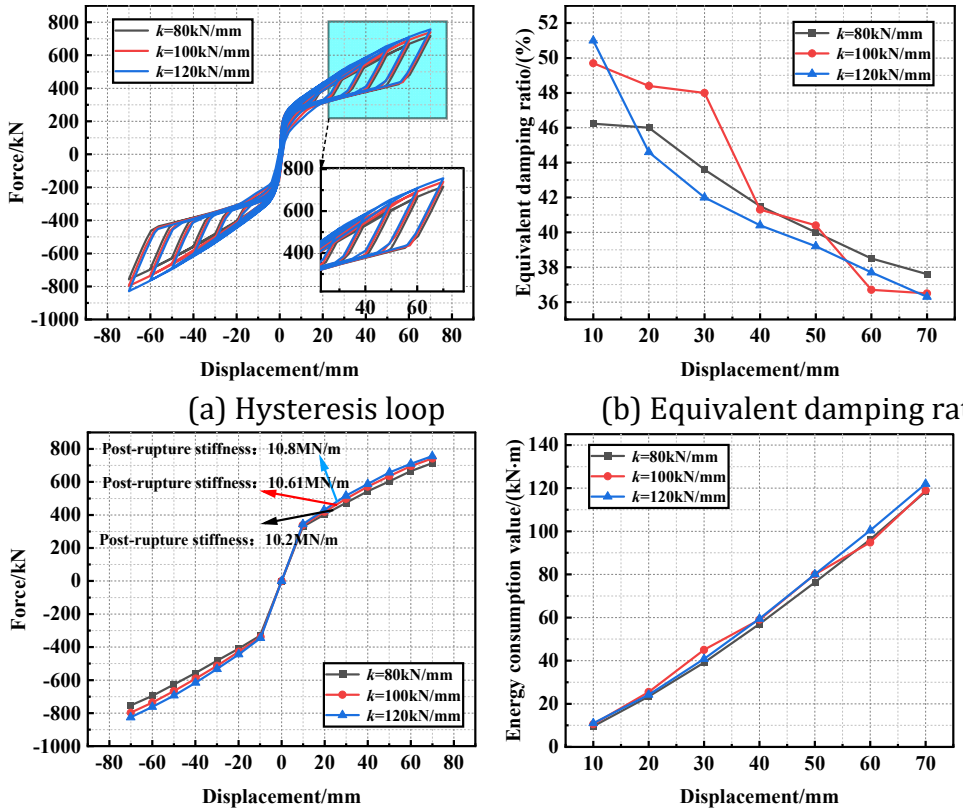

(a) Hysteresis loop (b) Equivalent damping ratio

(c) Skeleton curve (d) Comparison of energy dissipation values

Figure 11. Comparison of various parameters under different spring stiffness

5.3. The influence of the friction coefficient of the damper

Figure 12 shows the force-displacement curves, equivalent damping ratios, hysteretic energy dissipation values and residual displacements of the bridge piers under lateral cyclic loads at different displacement amplitudes when the initial tension stress of the prestressed tendons is 850 MPa and the stiffness of the damper spring is 120 kN/mm.

The friction coefficients μ between the damper slider and the V-shaped friction plate are 0.2, 0.23 and 0.25 respectively. When the friction coefficient of the damper increases from 0.2 to 0.23, the maximum restoring force increases by 0.23%, the equivalent damping ratio of the structure at the maximum displacement decreases by 0.6%, the energy dissipation value increases by 3.6%, and the residual displacement increases by 9.9%. When the friction coefficient of the damper increases from 0.23 to 0.25, the maximum restoring force increases

ISSN: 2710-0588

by 0.87%, the equivalent damping ratio of the structure at the maximum displacement decreases by 0.2%, the energy dissipation value increases by 0.67%, and the residual displacement increases by 5.5%.

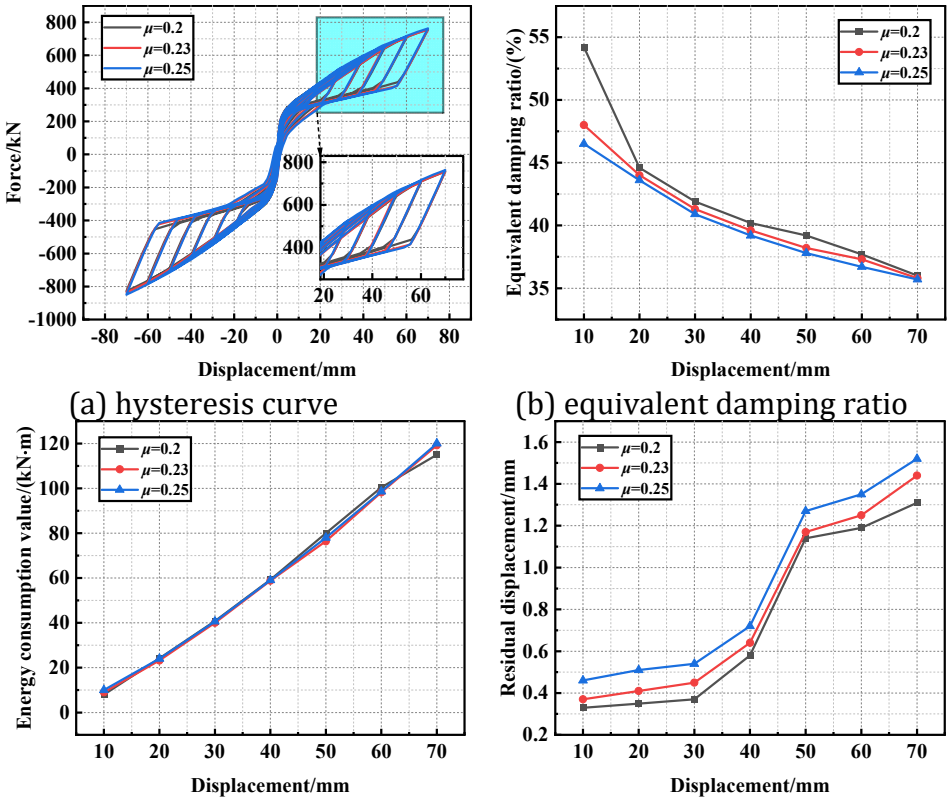

(a) hysteresis curve (b) equivalent damping ratio

(c) Energy consumption comparison (d) Residual displacement comparison

Figure 12. Comparison of various parameters under different friction coefficients

6. Conclusion

To enhance the energy dissipation capacity and seismic performance of the double-column swaying bridge piers with prestressed tendons, this paper proposes a system of adding VFSCD (Variable Frictional Coefficient Composite Self-resetting Dampers) to the double-column swaying piers. Firstly, the overall structure is introduced. Then, the force-displacement relationship of the VFSCD added to the double-column swaying piers is theoretically derived. The numerical calculation results are compared with the calculated results of the lateral load-bearing capacity formula derived from the theoretical analysis to verify the accuracy of the model. Finally, parametric analysis is conducted, and the following conclusions are drawn:

(1) After prestressed steel strands were added to the damping device of the double-column swaying bridge piers, the participation of the damping device enhanced the energy dissipation capacity of the bridge piers, increased the restoring force of the swaying bridge piers, made the hysteresis curve more full, and significantly improved the energy dissipation ability.

(2) The finite element software ABAQUS was utilized to conduct numerical calculations on the model of double-column swing abutment with damping devices added. The obtained results were basically consistent with those derived from the theoretical formulas, verifying the feasibility of adding self-resetting dampers in improving the seismic performance of swing abutments.

(3) Based on the parametric analysis, it can be concluded that when the initial prestress of the prestressing tendons, the stiffness of the damper spring, and the friction coefficient are larger, the restoring force generated by the bridge pier will also be greater. When the initial tension

ISSN: 2710-0588

stress applied to the prestressing tendons is 0.45 times the yield strength, the stiffness of the damper spring is 120 kN/mm, and the friction coefficient is 0.25, the system has good energy dissipation and self-resetting performance.

References

[1] Ramanathan K, Desroches R, Padgett J E. A comparison of pre- and post-seismic design considerations in moderate seismic zones through the fragility assessment of multispan bridge classes. Engineering Structures[J]. 2012; 45:559-573.

[2] Kawashima K, Macrae G A, Hoshikuma J.I, Nagaya K. Residual displacement response spectrum[J]. Journal of Structural Engineering. 1998.124:523-530.

[3] BECK J L S R I. The seismic response of a reinforced concrete bridge pier designed to step [J]. Earthquake Engineering & Structural Dynamics, 1973, 2(4): 343-358.

[4] G C L. The design and construction of the major bridges on the Mangaweka rail deviation [J].Transactions of the Institution of Professional Engineers New Zealand: Civil Engineering Section, 1988, 15(1): 17-23.

[5] ASTANEH-ASL A, SHEN J H. Rocking Behavior and Retrofit of Tall Bridge Piers; proceedings of the Structural Engineering in Natural Hazards Mitigation, F, 1993 [C].

[6] JIN S S,ZHOU S S,WAN X. Experiment on seismic performance of assembled piers with energy dissipation of replaceable corrugated steel plates[J/OL]. Journal of Jilin University (Engineering and Technology Edition), 1-11[2025-02-21].

[7] GU S. Study on seismic performance of self resetting piers with external viscoelastic dampers[D]. Jilin Jianzhu University,2024.

[8] Zhang J,Shen Y L.Seismic performance of prefabricated pier with replaceable damper[J]. Journal of Chongqing University,2023,46(02):98-106.

[9] LIU X R.Study on the anti-buckling support and seismic performance of continuous beam arch bridges[D].Central south University of Forestry and Technology,2023.

[10] LIU Y F,ZHANG W X,DU X L. Isolation effect and influence parameters of mass rotating wrap rope device for regular continuous girder bridge[J].Journal of vibration engineering, 2024,37(11):1818-1825.

[11] Xue D, Bi K M, Dong H H, et al. Development of a novel self-centering slip friction brace for enhancing the cyclic behaviors of RC double-column bridge bents [J]. Engineering Structures. 2021, 232: 111838.

[12] Hashemi, Ashkan, Zarnani, et al. Experimental Testing of Rocking Cross-Laminated Timber Walls with Resilient Slip Friction Joints[J]. Journal of Structural Engineering, 2018.

[13] XU L H, FAN X W, DAI C S, LI Z X. Mechanical behavior analysis and experimental study on pre-pressed spring self-centering energy dissipation brace[J]. Journal of Building Structures, 2016, 37(09): 142-148.

[14] Yu T H,Zhang C,Bao W. Mechanical performance analysis of a three-dimensional isolation device incorporating dis springs with U-shaped damper[J/OL].Building structre,1-7[2025-01-18]

[15] Pang W,Jiang H,Jia J F. Seismic design and numerical verification of self-centering double-column bridge with replaceable posttensioned strands[J/OL].Journal of Disaster Prevention and Mitigation Engineering.

[16] ASLAM M, GODDEN W G, SCALISE D T. Earthquake rocking response of rigid bodies [J]. Journal of the Structural Division, 1980, 106(2): 377-392.